PHYSICAL REVIEW B VOLUME 40, NUMBER 9 15 SEPTEMBER 1989-II

Lattice dynamics of quenched diffuse ω phase in $Zr_{0.8}Nb_{0.2}$

Y. Noda
Faculty of Engineering Science, Osaka University, Toyonaka, Osaka 560, Japan

Y. Yamada
Institute for Solid State Physics, The University of Tokyo, Roppongi, Minatoku, Tokyo 106, Japan

S. M. Shapiro
Brookhaven National Laboratory, Upton, New York 11973
(Received 5 August 1988; revised manuscript received 22 March 1989)

Phonon dispersion curves of the quenched diffuse ω phase of $Zr_{0.8}Nb_{0.2}$ have been measured along the [100], [001], [111], and [211] directions. Special attention was paid to the transverse-acoustic (TA) mode along the [211] and [011] directions in order to understand the structural and dynamical characteristics of the diffuse ω phase. In addition to the ordinary phonon branches, extra excitations forming subsidiary branches were observed for those TA modes, one of which had already been reported by Axe *et al.* In order to explain such anomalous behavior, we discuss the result in terms of the modulated lattice-relaxation model and the heterogeneous two-phase model.

I. INTRODUCTION

A number of alloys at the stability limit of a bcc structure (conventionally called Hume-Rothery alloys) undergo phase transitions from a bcc structure to various types of hexagonal-based structures including hcp and fcc. Phase transformations from the bcc phase to the ω phase are considered to belong to this case. Extensive studies of the ω phase were performed over the past two decades.[1] As is well known, the crystal structure of the ω phase is described by a collapse of neighboring pairs of (111) atomic planes of the bcc lattice. From the standpoint of lattice dynamics, this structure is considered to arise from a condensation of the TA_2 phonon mode with $\mathbf{q}=\frac{1}{3}(2,1,1)$ and $\mathbf{e}\|[\bar{1}11]$ or, equivalently, the LA mode with $\mathbf{q}=\frac{2}{3}(1,1,1)$ as shown in Table I.

In the table, we also include "soft modes" associated with the martensitic transformations in order to demonstrate the close relationship between the ω phase and martensitic phases.[1-7] Martensites belonging to the $9R$ structure are one of the typical examples in which the TA_2-phonon branch along the [110] direction is the relevant mode for the transformation. For instance, the martensitic transformation of the Ag-Zn alloy was interpreted[7] by the simultaneous condensations of two TA modes at $\mathbf{q}=\frac{1}{3}(1,1,0)$ and $\frac{1}{3}(2,1,1)$, in which the characteristic features of the atomic displacements were given by the rotational displacements in the basal plane and collapse of pairs of (111) atomic planes. In Fig. 1, unstable points in the reciprocal space of a bcc crystal are shown. The figure indicates the (111) reciprocal plane including [211] and [110] directions. One will easily notice that the relevant phonon modes for martensitic transformations and also the ω phase locate on this reciprocal plane and have a close relationship to each other. The F point in the figure is the so-called ω point, while the Γ-N line is the unstable line for the martensitic transformations. However, we should bear in mind that the so-called ω-phase transformation cannot be defined as clearly as in the case of martensitic transformation. The ω phase is obtained by quenching a β-based alloy as a metastable state and is usually coexisting with the bcc matrix in the form of small particles.

From the viewpoint of the diffraction experiment, the ω phase shows up as characteristic reflections observable around $(\frac{2}{3},\frac{2}{3},\frac{2}{3})$ positions in the bcc reciprocal lattice (F point in Fig. 1), and the width of the reflection strongly depends on the concentration as well as the heat treatments of alloys; some materials give sharp peaks and others diffuse peaks.[8-11] The quenched material, which gives peaks with a large width, is usually called the "diffuse ω phase" or "athermal ω phase." When the diffuse ω phase is annealed for a long time, the diffuse peaks become very sharp (aged ω phase). However, it has not been established yet whether the long-range ordering of the ω phase takes place as a homogeneous stable "phase" or not.

The lattice-dynamical properties of the ω phase are also extraordinary. Moss *et al.*[11] and Axe *et al.*[12] performed neutron-scattering experiments of $Zr_{0.8}Nb_{0.2}$ and $Zr_{0.92}Nb_{0.08}$ alloys and measured the phonon dispersion of the TA_2[211] mode in order to investigate the behavior of the relevant soft phonons in the bcc phase. $Zr_{1-x}Nb_x$ is one of the typical examples having the ω phase at room temperature. They found that in the bcc phase at $T=965\,^{\circ}C$ the spectra of the TA_2[211] mode are very anomalous; the TA_2 branch apparently splits into two subbranches. This means that if we count the subbranches as two different modes, there arises an inconsistency between the number of the modes and the number of degrees of freedom in the bcc structure. Such an anomalous feature has been tentatively interpreted in

TABLE I. Hexagonal-based structures induced by instability of body-centered-cubic structure and associated soft modes.

Low-temperature structure	Associated soft mode Direction	q		e	Position in Fig. 1
ω phase	[211]	$\frac{1}{3}$	TA_2	[111]	F
	[111]	$\frac{2}{3}$	LA	[111]	F
$2H$ martensite	[110]	$\frac{1}{2}$	TA_2	$[\bar{1}10]$	N
	[211]	$\frac{1}{2}$	TA_2	$[\bar{1}11]$	N
$9R$ martensite	[110]	$\frac{1}{3}$	TA_2	$[\bar{1}10]$	Along Σ
	[110]	0 $[C'=\frac{1}{2}(C_{11}-C_{12})]$	TA_2	$[\bar{1}10]$	Along Σ
	[211]	0 (C_s mode in Ref. 2)	TA_2	$[\bar{1}11]$	Along F

terms of the heterogeneous inclusion of ω-phase particles in the bcc matrix.

On the other hand, Yamada *et al.*[13–16] recently proposed a model called the MLR (modulated lattice relaxation) model concerning the structure of the premartensitic state of bcc-based alloys. This model assumes existence of an "embryo" (atomic cluster which locally simulates the low-temperature martensite structure), which thereby induces strain fields within the crystal in the premartensite state. Since there is a close relationship between the ω phase and the premartensitic state,[1,6] we consider that the so-called diffuse ω phase may also be in the MLR state, and the anomalous feature of the phonon dispersion observed in ZrNb alloys may be understood as one of the lattice-dynamical characteristics of the MLR lattice. In the present investigation we extended the previous study[12] to lower temperatures in the diffuse ω phase, since the "symmetry breaking" is the most important point in understanding the structural characteristics of the ω phase.

In addition to the reexamination of the $TA_2[211]$ mode of $Zr_{0.8}Nb_{0.2}$, we observed the $TA_1[211]$ ($\mathbf{e}\|[01\bar{1}]$) and LA[211] branches for comparison. Measurements of $TA_2[110]$ ($\mathbf{e}\|[\bar{1}10]$) and LA[111] phonon branches were also carried out since these branches are relevant to the phonon instabilities of the bcc phase (see Fig. 1 and Table I).

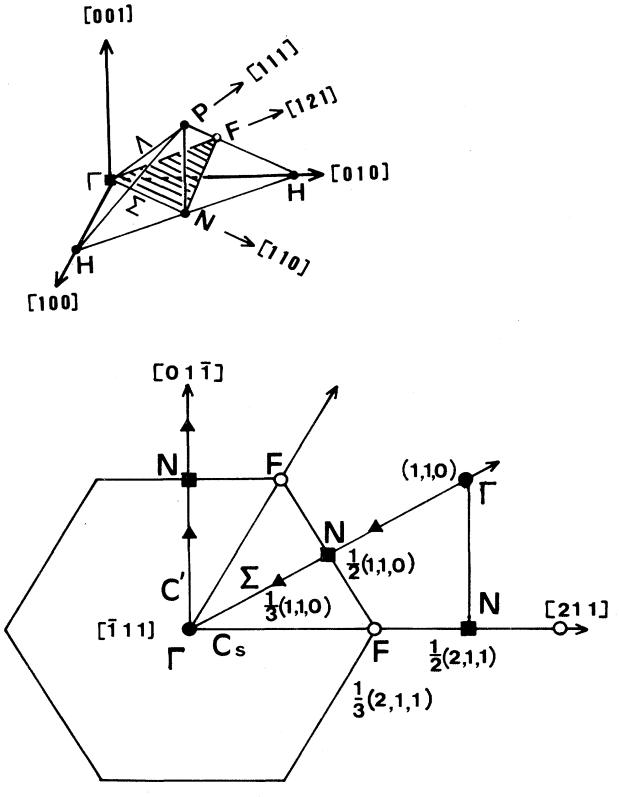

FIG. 1. A particular zone of reciprocal space which includes the q vectors relevant to the phase transitions of the bcc structure. In the text, the $\frac{1}{3}(2,1,1)$ position is expressed as the "F point" instead of the special position on the "F line."

II. EXPERIMENT

Neutron-scattering measurements of the $Zr_{0.8}Nb_{0.2}$ alloy were performed on a triple-axis spectrometer at the high-flux beam reactor of the Brookhaven National Laboratory. The single crystal of $Zr_{0.8}Nb_{0.2}$ was the same one used in previous studies[11] and was approximately cylindrical (13 mm diameter×20 mm height) in shape. It has a mosaic spread of 0.3° full width at half maximum (FWHM). Several scattering planes were used to measure the phonon branches along the [100], [011], [111], and [211] directions by remounting the same crystal. All of the experiments were performed at room temperature.

The spectrometer configurations used here employed pyrolytic graphite (002) as the monochromator and the analyzer. Both constant-Q scans and constant-E scans, with fixed final energy E_f, were used to measure the phonon spectra. Several combinations of E_f and collimation were used according to the experimental conditions; for instance, $E_f=14.7$, 30.5, and 41.0 meV, and collimations of 20′-10′-10′-20′ to 40′-20′-20′-40′. A pyrolytic-graphite filter between the sample and the analyzer was used to

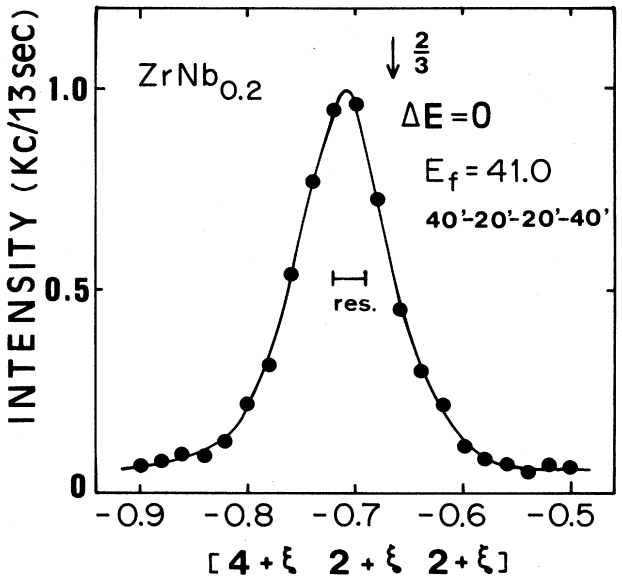

FIG. 2. Diffuse scattering around $Q=(\frac{10}{3},\frac{8}{3},\frac{8}{3})$. Instrumental resolution is shown by the horizontal bar. The peak position for the commensurate structure is indicated by the arrow.

reduce the higher-order contamination of the incident beam.

Quenched $Zr_{0.8}Nb_{0.2}$ has a bcc structure with the lattice constant $a=3.52$ Å. In order to characterize our sample, we measured the elastic diffuse scattering around $(H,K,K)\pm(\frac{2}{3},\frac{2}{3},\frac{2}{3})$. As shown in Fig. 2, the observed spectra are significantly broadened and the peak positions shift from the exact $(\frac{2}{3},\frac{2}{3},\frac{2}{3})$ positions in the reciprocal space. These characteristics are consistent with the previously investigated diffuse ω phase.[8-11] In the present experiment, we concentrate on the measurement of the lattice-dynamical behavior of the diffuse ω phase.

III. EXPERIMENTAL RESULTS

Phonon-dispersion curves have been measured along the [100], [011], [111], and [211] directions. Well-defined phonon peaks were obtained for these branches, except for two transverse-acoustic modes: the $TA_2[011]$ ($e\|[0\bar{1}1]$) and $TA_2[211]$ ($e\|[\bar{1}11]$) modes. Shown in Fig. 3 are the observed phonon dispersion curves where the well-defined peak positions of the spectra are shown by the solid circles. The solid line in the figure is drawn as a guide to the eye. The open circles and the ellipses on the $TA_2[011]$ and $TA_2[211]$ branches are the peak positions roughly estimated from the phonon spectra which have remarkably anomalous features. Examples of the $TA_2[011]$ phonon spectra at the momentum transfer $q=0.2$, 0.35, and 0.5 are shown in Fig. 4. At the smaller-q region and at the zone boundary, the phonon spectra seem to be normal. When the momentum transfer reaches $q\sim\frac{1}{3}$, the spectrum becomes anomalously broad and sometimes shows double peaks. In Fig. 3, we expressed the anomalous broadening on the $TA_2[011]$ branch with the vertical bar indicating the FWHM of the spectrum.

The phonon spectra of the $TA_2[211]$ mode are much more complicated. The profile of the spectrum is very broad and changes from Brillouin zone to Brillouin zone. The peak position, and hence the phonon dispersion curve itself, changes from zone to zone. This anomalous behavior in the $Zr_{0.8}Nb_{0.2}$ alloy observed at room temperature is essentially the same as the feature reported by

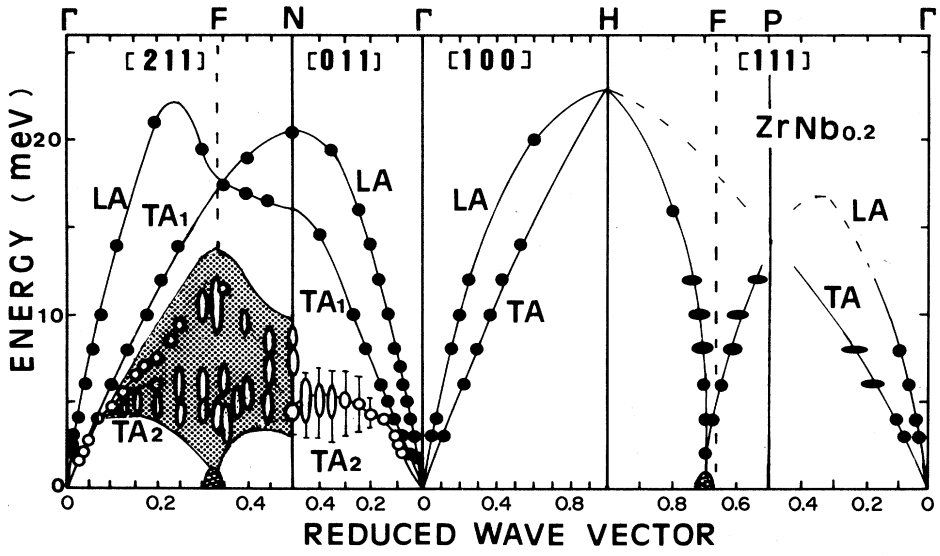

FIG. 3. Phonon dispersion curves of $Zr_{0.8}Nb_{0.2}$ observed at room temperature. Solid circles are the phonon energies of well-defined peaks, while the open ellipses are peak positions which can only be roughly estimated. Vertical bars give the FWHM of the broad spectra. The shaded area represents the existence of the anomalous phonon response.

Axe *et al.*[12] in the high-temperature bcc phase of $Zr_{0.92}Nb_{0.08}$. We have extended their experiments to a wider region in reciprocal space and observed the spectra more precisely in the diffuse ω phase.

Figure 5 shows the example of the $TA_2[211]$ phonon spectra around the (222) Bragg reflection; one is for the $[\bar{2}11]$ direction and the other is for the $[2\,\bar{1}\,\bar{1}]$ direction. At the small-momentum-transfer region ($q<0.1$), well-defined phonon peaks are observed for both directions. When the q value goes beyond this region and approaches $q=\frac{1}{3}$, the phonon spectra become very broad and split into double peaks. Around $\mathbf{Q}=(\frac{4}{3},\frac{7}{3},\frac{7}{3})$, that is, $(2,2,2)+\frac{1}{3}(\bar{2},1,1)$, the intensity of the lower-energy peak is stronger than that of higher energy, while the higher-energy peak is stronger than the lower-energy one around $\mathbf{Q}=(\frac{8}{3},\frac{5}{3},\frac{5}{3})$ $[(2,2,2)-\frac{1}{3}(\bar{2},1,1)]$. The overall phonon spectra have the following characteristics: the higher subbranch is dominant on $\mathbf{Q}=[222]+q[2\,\bar{1}\,\bar{1}]$ and the lower subbranch becomes dominant on $\mathbf{Q}=[222]+q[\bar{2}11]$ for $0.2<q<0.5$. We made observations at different zones to check this point. Figure 6 shows the spectra for the $TA_2[211]$ mode observed on the line between (222) and (033) Bragg reflections. Here we used the poor resolution of $E_f=41$ meV and 40′-20′-20′-40′ collimations in order to reach to the (033) Bragg reflection. Again, the higher branch becomes dominant on $\mathbf{Q}=[033]+q[2\,\bar{1}\,\bar{1}]$.

In Fig. 7 we summarized the observed phonon dispersion curves of the $TA_2[211]$ mode. Solid ellipses in the figure give roughly estimated peak positions of the dominant branch, and the open ellipses are for the weaker peaks or the subsidiary branches. The vertical bars are not the error bars, but instead indicate the FWHM of the spectra. The inset of the figure gives the direction (shown by the solid line) along which we measured the $TA_2[211]$ phonon mode. The F points are the so-called ω points where the quasielastic diffuse scattering peaks are observed. A strong diffuse peak is observed at $\mathbf{Q}=(\frac{4}{3},\frac{7}{3},\frac{7}{3})$, as shown by the large solid ellipsis in Fig. 7, and weak diffuse peaks at $\mathbf{Q}=(\frac{8}{3},\frac{5}{3},\frac{5}{3})$ and $(\frac{2}{3},\frac{8}{3},\frac{8}{3})$, as indicated by small solid ellipses in the figure. In Fig. 3 we folded these two subbranches and expressed by the shadowed broad

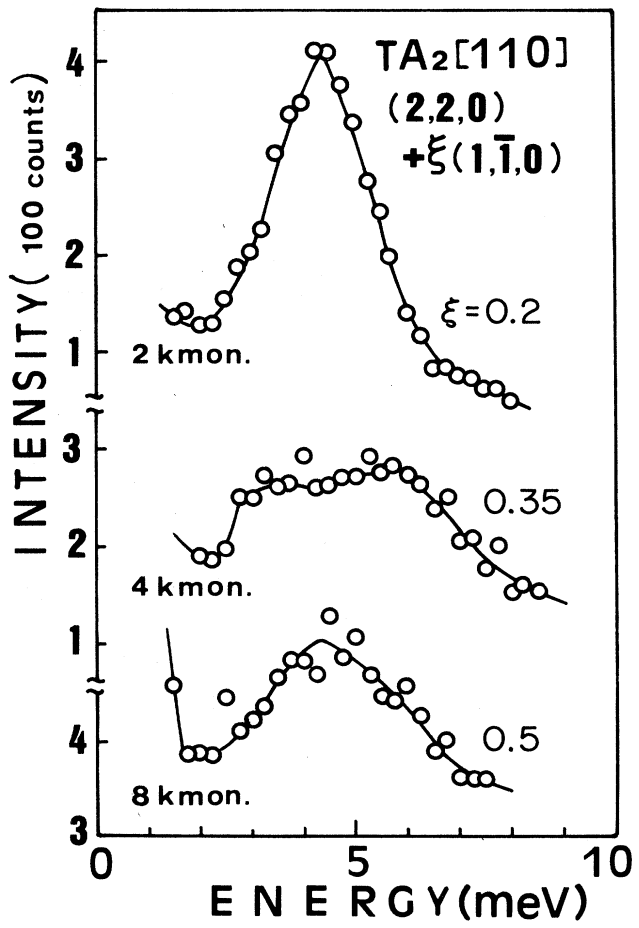

FIG. 4. Phonon spectra of the $TA_2[110]$ mode around (220) Bragg reflection observed by the condition of $E_f=30.5$ meV with 40′-20′-20′-40′. 2kmon. stands for 2000 monitor counts and corresponds to about 1 min of counting time.

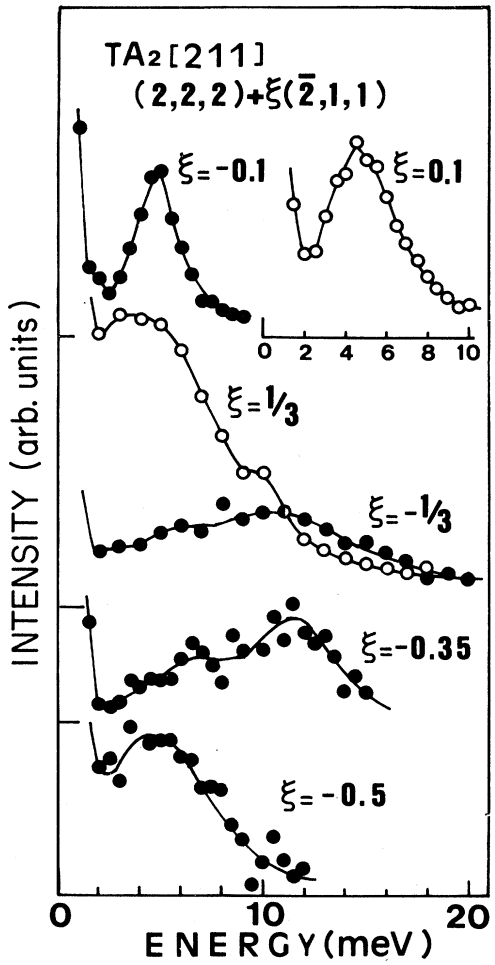

FIG. 5. Phonon spectra of the $TA_2[211]$ mode around (222) Bragg reflection. Data between $(3,\frac{3}{2},\frac{3}{2})$ and $(1,\frac{5}{2},\frac{5}{2})$ are taken by the condition of $E_f=30.5$ meV with 40′-20′-20′-40′ collimation.

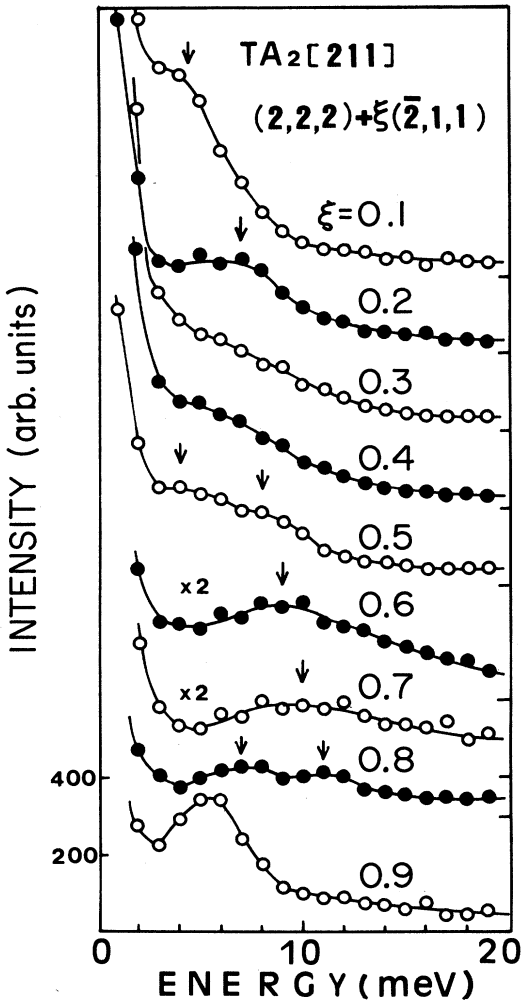

FIG. 6. Phonon spectra of the $TA_2[211]$ mode at the q value lying between the (222) and (033) Bragg reflections observed under the conditions of $E_f=41$ meV with 40′-20′-20′-40′ collimation.

band the overall phonon response of the $TA_2[211]$ mode. The open ellipses indicate the two subbranches within the wide band.

The LA[111] phonon spectra around the F point were measured by the constant-E-scan method. Examples of the spectra observed at the relatively low-energy regions are shown in Fig. 8. Since the dispersion curve around the F point is extremely steep, the splitting of two phonon peaks is not so clear. We only estimated the peak positions as indicated by arrows in the figure. The measurement of phonon peaks between $E=2$ and 0 meV was difficult, and failed because the present resolution function could not separate the influence of the strong intensity originating from the diffuse scattering of the F point.

IV. ELASTIC CONSTANTS

There are only three elastic constants in a cubic system: C_{11}, C_{12}, and C_{44}. In this section we discuss the elastic constants derived by measuring the velocity of

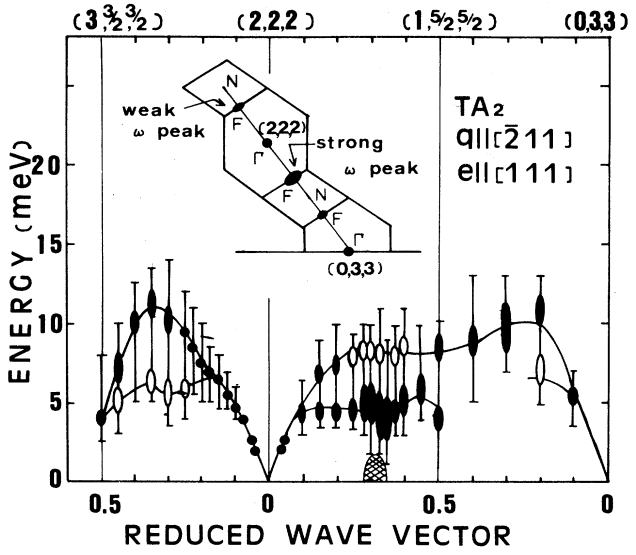

FIG. 7. Observed $TA_2[211]$ phonon branches. Solid ellipses and open ellipses represent the stronger and weaker peak positions, respectively. Cross-hatched areas on the horizontal axis ($\omega=0$) represent quasielastic response. The inset gives the direction along which the observations were carried out.

sound along several symmetry directions of the $Zr_{0.8}Nb_{0.2}$ alloy. By solving the equations of motion of the atoms responding to the forces acting on the crystal,[17] effective elastic constants are obtained and shown in Table II. Here, the acoustic phonons along the [100], [110], and [111] directions are purely longitudinal and transverse, while only the TA_1 mode has pure transverse character along the [112] direction. The elastic constants C_+ and C_- in the table are the following:

$$C_\pm=\tfrac{1}{12}\{(5C_{11}+C_{12}+8C_{44}) \pm[(3C_{11}-C_{12}-4C_{44})^2-32(C_{12}+C_{44})^2]^{1/2}\} .$$

The displacements of these two phonon modes are expressed as $\mathbf{e}_+$ and $\mathbf{e}_-$ in the table and are solved as follows:

$$\mathbf{e}_+=(1,1,[3C_+-\tfrac{1}{2}(C_{11}+C_{12}+6C_{44})]/(C_{12}+C_{44})) ,$$

$$\mathbf{e}_-=(1,1,2(C_{12}+C_{44})/[3C_--(2C_{11}+C_{44})]) .$$

Thus, $\mathbf{e}_+$ and $\mathbf{e}_-$ are not necessarily parallel or perpendicular to the [112] direction and will change with the change of the values of C_{11}, C_{12}, and C_{44}. In the table we listed the values of effective elastic constants where C_{11} are calculated from the slope of the LA[100] mode, C_{44} from the TA[100] mode, and C_{12} from the TA[111] mode. Other effective elastic constants are calculated from these elastic constants and show good consistency with the observed slopes of the phonons in $Zr_{0.8}Nb_{0.2}$.

The question is how pure are the LA[112] and $TA_2[112]$ modes? The calculated displacement directions, from the values C_{11}, C_{12}, and C_{44} given in Table II, are $\mathbf{e}_+=(1,1,1.86)$ and $\mathbf{e}_-=(1,1,-1.08)$. Consequent-

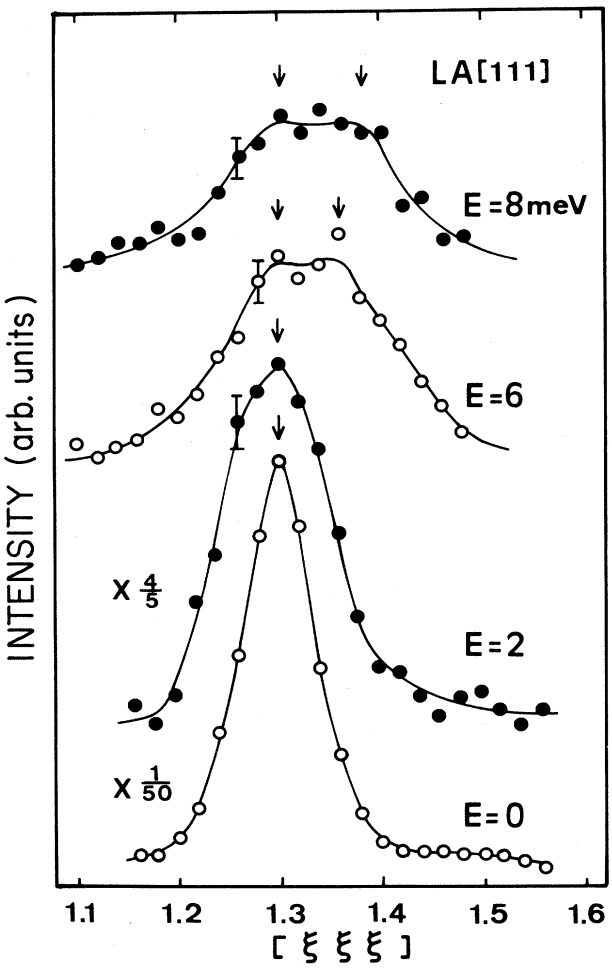

FIG. 8. Phonon spectra of the LA[111] mode around the F point measured by the constant-E-scan method. Condition of the spectrometer is $E_f = 30.5$ meV with 40′-20′-20′-40′ collimation.

ly, these two phonon modes are very close to the pure longitudinal and transverse modes in the $Zr_{0.8}Nb_{0.2}$ system. However, it should be emphasized that the displacement vectors can change when the elastic constant $\frac{1}{2}(C_{11}-C_{12})$ tends to zero.

Finally, we compare the C_- mode with the so-called special mode C_s described by Nagasawa *et al.*[2] The elastic constant C_s is defined as

$$C_s=\tfrac{1}{2}(C_{11}-C_{12})+3C_{11}+5C_{12}$$
$$+2C_{44}[C_{44}-\tfrac{1}{2}(C_{11}-C_{12})](C_{11}+C_{12})\ .$$

The direction of this TA mode is close to the [112] direction, but not exactly on the [112] line. This mode is defined as the lowest phonon surface of the TA mode between the [110] and [001] directions. Therefore, it is slightly different from our expression of the TA_2[112] or the C_- mode. In this paper, we mainly discussed the phonon dispersion curve along the symmetry directions including the [112] direction. In this sense, the C_- elastic constant is much more convenient to compare with the present neutron-scattering experiments.

V. DISCUSSIONS AND CONCLUSION

We measured the phonon dispersion curves of the $Zr_{0.8}Nb_{0.2}$ alloy in the diffuse ω phase at room temperature (Fig. 3). Overall features of the lattice dynamics are similar to those in pure Zr metal and $Zr_{0.92}Nb_{0.08}$ alloys, which were given in the previous reports.[12,18,19] The LA[211] and TA_1[211] phonon branches are newly obtained, which are important to compare with the TA_2[110] branch. These two phonon branches do not show any anomalous behavior. We have observed anomalous broadening of the TA_2[110] phonon mode, which is the relevant mode for martensitic transformations. We point out that this branch has a compatibility relation to

TABLE II. Effective elastic constants in $Zr_{0.8}Nb_{0.2}$. $e_\pm$ and $C_\pm$ are shown in text. The density of the crystal is 7.0 g/cm^3 and the unit of the elastic constant is 10^{12} dyn/cm^2. Data of Zr at 1400 K are taken from Refs. 18 and 19.

q	e	Elastic constant	$Zr_{0.8}Nb_{0.2}$	Zr(1400 K)
[100]LA	[100]	C_{11}	1.6	1.1
TA	[010]	C_{44}	0.4	0.3
		C_{12}	1.1	0.9
[110]LA	[110]	$\frac{1}{2}(C_{11}+C_{12}+2C_{44})$	1.7	1.3
TA_1	[001]	C_{44}	0.4	0.3
TA_2	[$\bar{1}$10]	$\frac{1}{2}(C_{11}-C_{12})$	0.3	0.1
[111]LA	[111]	$\frac{1}{3}(C_{11}+2C_{12}+4C_{44})$	1.7	1.3
TA	[1$\bar{1}$0]	$\frac{1}{3}(C_{11}-C_{12}+C_{44})$	0.3	0.1
[112]LA	e^+	C_+	1.7	
TA_2	e_-	C_-	0.3	
TA_1	[110]	$\frac{1}{6}(C_{11}-C_{12}+4C_{44})$	0.3	

the $TA_2[211]$ phonon branch at the zone-boundary N point.

The deep dip of the LA[111] phonon mode was also observed near the F point. This anomalous behavior of the LA[111] mode is one of the characteristic features of bcc alloys. However, we should note that the deepest point of the LA[111] mode in the ω phase slightly shifts from the exact F point to the position of the diffuse ω spot. Since the LA[111] phonon mode of the F point has a compatibility relation to the $TA_2[211]$ mode at this particular point, we consider that the existence of the energy gap between the deepest point of the LA[111] mode and the quasielastic part of the diffuse scattering shown in Fig. 3 is not so clear, but rather we conjecture that there is a sheetlike response reaching to the diffuse spot.

The most remarkable characteristic of the observed phonon spectra of the diffuse ω phase is that there seems to be extra excitations in the $TA_2[211]$ mode, so that the TA branch looks as if it splits into two—the main branch and the subsidiary branch. This extraordinary characteristic was already pointed out and studied by Axe *et al.*[12] on the same alloy with a different concentration of $Zr_{0.92}Nb_{0.08}$. Axe *et al.* considered that even at the elevated temperatures well within the bcc phase field there is ω-like static short-range order. The cubic symmetry of the system is broken at least locally. This gives the essential reason for the apparent inconsistency between the number of branches and the degree of freedom of the atoms in the bcc system.

More specifically, the interpretation of Axe *et al.* for the split branch is as follows: Since the F point becomes a new Bragg position in the ω phase, there should be a long-wavelength fluctuation corresponding to the TA branch even in the short-range-ordered ω particle. The observed low-energy response around $\mathbf{q}\sim\frac{1}{3}(2,1,1)$ is due to the excitations of the TA modes around the diffuse Bragg reflections at $\mathbf{q}=\frac{1}{3}(1,1,1)$, while the higher branch is ascribed to the response of the original bcc phonon branch.

In connection with the heterogeneity of the sample, it is suggestive that recent measurements with high-resolution electron microscopy reveal the existence of well-defined ω particles in a TiMo crystal when the sample is annealed for a long time (aged ω phase).[18] The spacing of the lattice image of the four types of ω variants, *a*, *b*, and *c*, are explained by the condensation of the phonon mode $TA_2[211]$ at $\mathbf{q}=\frac{1}{3}$, LA[111] at $\mathbf{q}=\frac{2}{3}$, and the [110] at $\mathbf{q}=0$ of a bcc lattice. The typical size of a variant is about 20×20 atomic units. In this case, the diffraction profile of the ω peak (F point) becomes very sharp. On the other hand, in the quenched samples (diffuse ω phase) the lattice image of the electron microscopy is smeared out and there is no clear ω particle observed. Our sample of $Zr_{0.8}Nb_{0.2}$ definitely corresponds to the latter case.

We follow essentially the same viewpoint in that the inconsistency of the number of branches is due to local symmetry breaking. However, we present an alternative interpretation of the origin of the split branches. Whereas both we and Axe *et al.* ascribe portions of the scattering to ω phase embryos, we differ in the interpretation of the fluctuation spectrum of these embryos. In the previous work Axe *et al.*[12] assumed the phonon frequency at $\mathbf{q}=\frac{1}{3}(2,1,1)$ [or $\frac{2}{3}(1,1,1)$] of pure bcc phase (without diffuse ω phase) to be that of bcc Nb (data for bcc Zr were not available). Recent observations on bcc Zr (Refs. 19–21) show this phonon frequency to be lower in bcc Zr than in bcc Nb and to contain appreciable quasielastic response.

We assume that the $TA_2[211]$ phonon branch of the pure bcc matrix itself shows intrinsic softening at $\frac{2}{3}(1,1,1)$. We suggest that the lower subbranch represents the response of the pure bcc phase, leaving the upper feature as due to the effect of the fluctuations in the ω phase. Basically the same structural model was developed by Cook[22] in the specific case of ω-phase fluctuations. The quasistatic structure with a MLR in the bcc matrix would be visualized as in Fig. 9 (also see Fig. 3 of Ref. 22). There is an extended region which simulates the static ω structure embedded coherently in the bcc matrix. The local potential $V(Q)$ (where Q is an ω-like dispacement) for this particular local displacement mode should have metastable states at $Q=Q_0$ as well as at $Q=0$. (This feature is demonstrated by first-principles calculations by Ho *et al.*[23]) Then the vibrational spectrum from the MLR embryo would have two characteristic frequencies corresponding to the potential around $Q=0$ and $Q=Q_0$. We consider that the latter is associated with observed upper subbranch, while the former is naturally associated with the lower branch.

At the present stage, the proposed dynamical MLR model is an alternative to the model of Axe *et al.* to interpret the anomalous features of the TA_2 mode in the ZrNb alloy. The model of Axe *et al.* does provide a reasonably quantitative explanation of the intensity variation in the subbranches. It is important to test whether the model we propose is capable of a better quantitative description. Further investigations on this point are in progress.

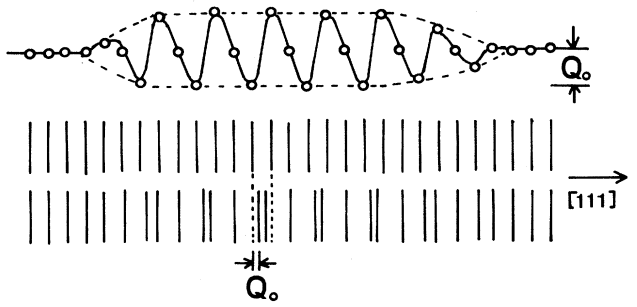

FIG. 9. Schematic representation of the MLR (embryonic fluctuation) embedded coherently on the matrix. The displacement pattern simulates the ω structure. Actually, the direction of the shift of atoms should be parallel to the propagation vector.

ACKNOWLEDGMENTS

We are indebted to Dr. J. D. Axe of Brookhaven National Laboratory and Professor S. C. Moss of the University of Houston for discussions and loan of the crystal, and to Professor M. Hida of Okayama University and Dr. K. Fuchizaki of Osaka University for many fruitful discussions. Work at Brookhaven National Laboratory was supported by the Division of Material Sciences, U.S. Department of Energy, under Contract No. DE-AC02-76CH00016, and carried out as part of the U.S.-Japan Neutron Scattering Collaboration Program.

[1]For a review, see B. S. Hickman, J. Mater. Sci. **4**, 554 (1969); also see S. K. Sikka, Y. K. Vohra, and R. Chidambaram, in *Progress in Material Science,* edited by B. Chalmers, J. W. Christian, and T. B. Massalski (Pergamon, New York, 1982), Vol. 27, p. 245.

[2]A. Nagasawa, N. Nakanishi, and K. Enami, Philos. Mag. **43**, 1345 (1981).

[3]M. Iizumi, J. Phys. Soc. Jpn. **52**, 549 (1983).

[4]S. K. Satija, S. M. Shapiro, M. B. Salamon, and C. M. Wayman, Phys. Rev. B **29**, 6031 (1984).

[5]S. Vatanayon and R. F. Hehemann, in *Shape Memory Effect in Alloys,* edited by J. Perkins (Plenum, New York, 1975), p. 115.

[6]S. M. Shapiro, Y. Noda, Y. Fujii, and Y. Yamada, Phys. Rev. B **30**, 4314 (1984).

[7]Y. Yamada and Y. Noda, J. Phys. Soc. Jpn. **57**, 1303 (1988).

[8]W. Lin, H. Spalt, and W. B. Batterman, Phys. Rev. B **13**, 5158 (1976).

[9]H. Terauchi, K. Sakaue, and M. Hida, J. Phys. Soc. Jpn. **50**, 3932 (1981).

[10]N. Wakabayashi, Phys. Rev. B **17**, 387 (1978).

[11]S. C. Moss, D. T. Keating, and J. D. Axe, in *Phase Transitions–1973,* edited by L. E. Cross (Pergamon, New York, 1973), p. 179.

[12]J. D. Axe, D. T. Keating, and S. C. Moss, Phys. Rev. Lett. **35**, 530 (1975).

[13]Y. Yamada, Y. Noda, M. Takimoto, and K. Furukawa, J. Phys. Soc. Jpn. **54**, 2940 (1985).

[14]Y. Yamada, Y. Noda, and M. Takimoto, Solid State Commun. **55**, 1003 (1985).

[15]Y. Yamada, *Proceedings of the International Conference on Martensitic Transformations* (The Japan Institute of Metals, Sendai, 1986), p. 89.

[16]Y. Yamada, Metall. Trans. **19A**, 777 (1988).

[17]C. Kittel, *Introduction to Solid State Physics,* 3rd ed. (Wiley, New York, 1976), p. 119.

[18]M. Hida and E. Sukedai (unpublished).

[19]C. Stassis, J. Zarestky, and N. Wakabayashi, Phys. Rev. Lett. **41**, 1726 (1978).

[20]C. Stassis and J. Zaretsky, Solid State Commun. **52**, 9 (1984).

[21]W. Petry, A. Heiming, J. Trampenau, and G. Vogl, in *Proceedings of the International Conference on Diffusion in Metals and Alloys, Balatonfüred, Hungary, 1988,* edited by F. J. Kedoes and D. L. Beke (Trans Tech, Aedermannsdorf, Switzerland, 1989).

[22]H. E. Cook, Phys. Rev. B **15**, 1477 (1977).

[23]K. M. Ho, C. L. Fu, and B. N. Harmon, Phys. Rev. B **29**, 1575 (1984).